ISSN 1814-4225 (print)
ISSN 2663-2012 (online)

UDC 534.24

doi: 10.32620/aktt.2025.6.01

Petro LUKIANOV, Sergii KARMAZIN

National Technical University of Ukraine
"Igor Sikorsky Kyiv Polytechnic Institute", Kyiv, Ukraine

NOISE OF ELASTIC THICKNESS VIBRATIONS OF A HELICOPTER BLADE INDUCED BY AERODYNAMIC LOADS

This study develops *a theoretical model of vibration-induced noise generation in helicopter blade elastic vibrations. Vibration and aerodynamic noises are generated during helicopter rotor rotation. Numerous studies have been conducted on aerodynamic noise, and a number of theories have been proposed. However, vibration noise has been mainly studied experimentally or modeled only by the ordinary mechanical vibrations of the blade as a single body—a beam or plate. This does not consider the blade's elastic deformations, which generate elastic sound waves inside the body. Until now, no model has mathematically described the transformation of elastic longitudinal and transverse waves arising inside an elastic blade into sound waves. These waves emerge from the blade and propagate into the air during elastic thickness vibrations, which are formed by variable deformations under the action of variable blade loads.* ***The research methods are based on*** *the analytical solution of the boundary value problem for the Navier-Cauchy equation, which is divided into four Helmholtz equations: one for the scalar potential and three for the vector potential. Elastic waves of the Love's wave type are studied, but for a finite-sized thin elastic plate. Limiting standing waves to only one direction is impossible for a helicopter rotor blade of finite sizes, since the blade has finite dimensions. Therefore, the following model of vibration noise generation was proposed: the blade is approximately replaced by a thin elastic plate, inside which elastic longitudinal and transverse waves arise, which are governed by Helmholtz equations. The general solution to these equations is found using the method of variable separation (Fourier method). The reflection and scattering issues of sound waves from the interface between an elastic body and air are not considered in this study.* ***Results and conclusions****. This paper proposes a new physical model of vibration-induced sound: vibration-induced sound is generated as a result of the emission of elastic longitudinal waves, which are emitted from inside an elastic blade outward into the air. An analytical solution of scalar and vector potentials in the form of standing sound waves was obtained for a boundary value problem with a known distribution of aerodynamic, time-harmonic loads on the blade surfaces. This solution allowed us to write expressions for normal stresses on the blade surface. Time-varying stresses transfer the energy of longitudinal standing sound waves, which emanate from the blade's center outward into the air. They are the source of vibration-induced noise. The expression for normal stresses on the blade surface contains derivatives of both scalar and vector potentials, i.e., it considers the influence of both longitudinal and transverse waves. Thus, both wave types implicitly participate in the formation of normal stresses on the blade surface. The periodic change in these stresses over time causes periodic blade thickness deformation, which is the source of air acoustic vibrations. The calculated data for the longitudinal wave potential on the blade surface coincide with the well-known Gutin's theory of rotational sound: the maximum generated sound wave is located near the blade's outer end. This indicates that the analytical solution obtained in this work physically describes the vibration-induced noise generation process.*

Keywords: *vibration-induced noise model; aerodynamic load on helicopter blades; generation of elastic sound waves on helicopter blade surfaces.*

Introduction

Existing models of vibration-induced noise in helicopter blades are based on the vibration of the blade as a single solid body, i.e. in the approximation of the theoretical mechanics model, or it is assumed that the sound is caused by the bending vibrations of the blade, which are described by the Lagrange-Sophie Germain plate vibration equation. This raises the question: what exactly causes vibration-induced noise?

It is known that during the rotation of a helicopter rotor, two fundamentally different types of noise arise: noise of vibrational origin [1] and noise of aerodynamic origin [2]. These are two completely different types of noise. Noise of vibrational origin has been studied mainly experimentally. Gutin's model [1] is a simplified model: it considers sound emissions caused by mechanical vibrations of the blade under the action of an external load.

Creative Commons Attribution
NonCommercial 4.0 International

Let us consider the main existing models describing the sound of rotor blade rotation and its control with the aim of reducing it.Thus, in [3], a model is proposed that relates the aerodynamic characteristics of the blade to the resonance frequencies of the blade. One of the most common methods of reducing blade noise is individual blade pitch control (IBC) [4]. IBC is used to minimize noise and improve performance. In [5], a new device called smart pitch link is proposed, a device with superelastic material for passive vibration control. To achieve this goal, a shape memory alloy (SMA) is used.

One of the means of passive blade noise control is the use of blade trailing edge serration technology [6]. This approach reduces the noise generated when the flow leaves the blade at its trailing edge. This technology is presented in [7], which considers the use of modified double-wave saw-like serrations implemented on the trailing edge. This allows noise to be reduced by 3.3 dB. An experimental study [8] investigated the effect of changing the blade phase angle on the combined noise level of two propellers. It was found that at certain phase angles, noise can be reduced to 26 dB. Further experimental studies in this field [9] focus on the acoustic characteristics of overlapping propellers, with attention concentrated on the effect of transverse and axial separation under different flow conditions and propeller rotation speeds. Experimental studies are not always able to reveal the internal physical relationships and patterns of mutual influence between different types of noise. Therefore, theoretical research also continues. Thus, in [10], a theoretical and computational analysis of the differences between tonal and broadband noise was performed, which allows it to be used for preliminary propeller design. However, the theoretical studies listed above concern noise of aerodynamic origin. Noise of vibrational origin, as shown by the above analysis, has been studied mainly experimentally.

Today, another method of modeling helicopter blade noise is known, which is based on the equation of small plate vibrations. However, this approach is not perfect from the point of view of the physical model. We will present an analysis of works in this field, after which we will formulate the research objectives of this work.

1. Analysis of existing studies on blade vibration noise

Let us consider the existing models of vibration noise of a thin rectangular plate. In [11], the vibrations of an orthotropic plate are considered based on the bending equation of normal vibrations of a plate for a moving load. These vibrations include dependencies on the damping coefficient, boundary conditions, and speed of movement. In this case, the sound field is modelled based on the second derivative of the plate deflection. It is known that the equation of small plate deflections, obtained on the basis of a rigid plate model, allows for maximum deflections of this plate $w = h/5$, where h - is the plate thickness.

This model actually allows us to describe sound using small deflections of the plate: during the vibration of the plate, small changes in the amplitude of the plate deflection are considered to be the source of sound vibrations. But what if the blade deflections during screw rotation exceed this range? In this case, we are dealing with an elastic model of the blade, specifically the plate. And the amplitude of its deflection is no longer a small value. Therefore, it is no longer possible to consider sound as the source of these vibrations. Even in the first case, with small blade deflections, sound as such is not generated: the equation of plate bending vibrations is not a wave equation for a sound wave, i.e. it does not describe sound. Take, for example, an iron ruler and start to vibrate it perpendicular to the plane of the ruler. Can you hear a sound? No,you can not. You will only hear the rustling of air, i.e. its local fluctuations. Very often, hydromechanics mix up local air fluctuations with sound. These are not the same thing: local pulsations do not propagate at the speed of sound. However, if you press the ruler to a table and make it vibrate, the impact of the ruler on the table surface generates elastic waves inside the table surface, which we can hear.

In [12], the equation of bending vibrations of a plate is also used to model sound generation processes, taking into account incident and reflected waves. However, sound pressure is directly added to the plate vibration equation, on the right-hand side, as an external load. But this is not a physically correct model: the sound pressure is at least two orders of magnitude smaller than the usual plate displacements. And the equation for displacements is linear, with nonlinear terms, which are precisely small values, neglected in its derivation. In general, the equation for displacements can only include pressure caused by force loads on the blade, for example, aerodynamic forces. And sound pressure is too small in magnitude to be taken into account in the same equation with non-sound quantities. In [13], the external load is taken into account in the equation of bending vibrations in the form of a force applied to the plate.

In [14], a simplified one-dimensional non-stationary model of sound radiation is considered. In this case, the equation for modelling sound is a special case of the equation of bending vibrations of a plate, which, in the case of one variable, turns into the vibration of a rod. In [15], the problem of sound radiation by a plate under the influence of a random pressure pulsation field is solved. A non-resonant mechanism of sound radiation is considered. The

ISSN 1814-4225 (print)
ISSN 2663-2012 (online)

equation of vibrations of a plate in the form of a circular rib dividing infinite space is modelled by a bi-harmonic operator plus an inertial term, externally in the same way as for a rectangular plate. However, acoustic pressure is added to the equation in addition to the pressure generated on the surface of the plate. This is again a mistake: mechanical pressure and small perturbations cannot be written together in the equation. Sound is the result of vibrations and requires a separate equation. Once again, we see a lack of understanding of the difference between ordinary mechanical vibrations of a plate and sound vibrations. By the way, the speed of sound is completely absent from the plate vibration equation. So what sound are we talking about? An implicitly present one? This is an incorrect physical formulation. Work [16] describes an algorithm for calculating the acoustic radiation of a plate located in the field of wall-bounded turbulent pressure pulsations. This model describes the sound radiation of fuselage panels into the aircraft cabin.

Today, it is known that elastic Lamb waves are formed in an infinite elastic layer with two coordinates [17]. There are many works devoted to these waves [18, 19]. These waves emerge from the centre of this layer to its surface. Some of them are scattered, some return back, and some emerge into another acoustic medium [20]. The latter part of these waves actually forms the sound of vibrational origin. Since in this work we are considering not an infinite layer of finite thickness, but a helicopter blade, which is modelled as a thin rectangular plate of finite dimensions in three coordinates, a standing wave packet is formed in it.

Objective: To develop a theoretical model of vibration-induced noise in helicopter blade elastic vibrations and to perform a numerical calculation of the sound field potential in accordance with the suggested model.

2. Vibration noise model

Physical model. Let us approximate the blade with a thin rectangular elastic plate (Fig. 1), in which variable elastic normal deformations occur. In Kirchhoff-Love's hypotheses [21], on the basis of which the Lagrange-Sophie Germain equation was obtained, these deformations are neglected. Therefore, the Lagrange-Sophie Germain equation cannot describe the longitudinal sound waves that generate inside the plate.

It is known, for example, that thickness vibrations of piezoelectric transducers are a source of sound waves. It is the type of vibration caused by elastic deformations of the body that is the source of sound vibrations. Therefore, in this work, we will assume that vibration-induced noise is generated by the propagation of elastic waves from the body, the helicopter blade, into the surrounding environment – the air.

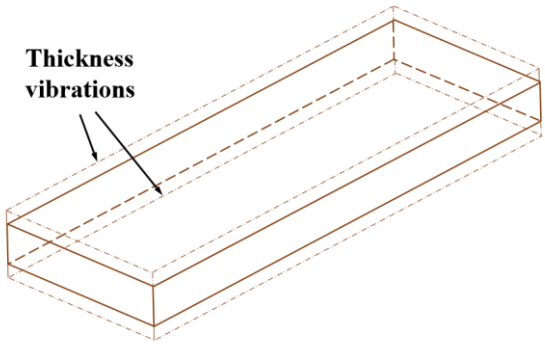

Fig. 1. Elastic vibrations of a helicopter blade

It is known that according to the hypothesis of small displacements and deformations, the existence of longitudinal and transverse sound waves inside an elastic body is governed by the Navier-Cauchy equation [22, 23]

$$\rho\ddot{\bar{u}} = (\lambda + 2\mu)\,\mathrm{graddiv}\bar{u} - \mu\,\mathrm{rotrot}\bar{u} \qquad (1)$$

where

$$\lambda = \frac{E\gamma}{(1+\gamma)(1-2\gamma)}, \mu = \frac{E}{2(1+\gamma)}.$$

The displacement vector $\bar{u}$ can be decomposed into longitudinal and transverse components:

$$\bar{u} = \bar{u}_l + \bar{u}_t. \qquad (2)$$

At the same time:

$$\mathrm{rot}\bar{u}_l = \bar{0}, \mathrm{div}\bar{u}_t = 0. \qquad (3)$$

Taking into account (2) and (3):

$$\rho\ddot{\bar{u}}_l + \rho\ddot{\bar{u}}_t = (\lambda + 2\mu)\,\mathrm{graddiv}\bar{u}_l - \mu\,\mathrm{rotrot}\bar{u}_t. \qquad (4)$$

In case of fulfilment (3), we can write:

$$\bar{u}_l = \nabla\varphi, \bar{u}_t = \mathrm{rot}\bar{\psi} \qquad (5)$$

and equation (1) will be transformed into two equations for scalar φ and vector $\bar{\psi}$ potentials:

$$\Delta\varphi + k_l^2\varphi = 0,\ \Delta\bar{\psi} + k_t^2\bar{\psi} = 0, \qquad (6)$$

where

$$k_l=\sqrt{\frac{\rho\omega^2}{(\lambda+2\mu)}},k_t=\sqrt{\frac{\rho\omega^2}{\mu}},\lambda=\frac{E\nu}{(1+\nu)(1-2\nu)},\mu=\frac{E}{2(1+\nu)}.$$

The first equation (6) describes longitudinal sound waves inside the blade, and the second describes transverse sound waves.

Hypothesis. Since the plate is thin, the intensity of sound waves emitted at the ends of the blade is significantly lower than the intensity of sound emitted by the upper and lower surfaces of the blade. Therefore, we will assume that the energy of elastic deformation under the action of a normal load on the plate is mainly spent on generating sound of vibrational origin during thickness vibrations of the blade. Thus, we neglect the lateral radiation at the ends of the blade.

3. Expressing stresses through scalar and vector potentials

Formula (5) expresses the vectors of longitudinal and transverse displacements through scalar and vector potentials, respectively. Taking into account (2), we have:

$$\bar{u}=\bar{u}_l+\bar{u}_t=\nabla\varphi+\mathrm{rot}\bar{\psi}. \qquad (7)$$

In the Cartesian coordinate system, the components of the displacement vector $\bar{u}$ on the axis x,y,z are written as [20]:

$$\begin{aligned}u_x&=\frac{\partial\varphi}{\partial x}+\frac{\partial\psi_z}{\partial y}-\frac{\partial\psi_y}{\partial z},\\ u_y&=\frac{\partial\varphi}{\partial y}+\frac{\partial\psi_z}{\partial x}-\frac{\partial\psi_x}{\partial z}, \qquad (8)\\ u_z&=\frac{\partial\varphi}{\partial z}+\frac{\partial\psi_y}{\partial x}-\frac{\partial\psi_x}{\partial y}.\end{aligned}$$

The components of the stress tensor are expressed in terms of displacement as follows:

$$\sigma_{xx}=\lambda\Delta+2\mu e_{xx},\sigma_{yy}=\lambda\Delta+2\mu e_{yy},\sigma_{zz}=\lambda\Delta+2\mu e_{zz},$$

$$\sigma_{xy}=\mu e_{xy},\sigma_{zx}=\mu e_{xz},\sigma_{zy}=\mu e_{yz}, \qquad (9)$$

where

$$\Delta=e_{xx}+e_{yy}+e_{zz}=\frac{\partial u_x}{\partial x}+\frac{\partial u_y}{\partial y}+\frac{\partial u_z}{\partial z},$$

$$e_{yz}=\frac{\partial u_z}{\partial y}+\frac{\partial u_y}{\partial z},e_{zx}=\frac{\partial u_z}{\partial x}+\frac{\partial u_x}{\partial z},e_{xy}=\frac{\partial u_y}{\partial x}+\frac{\partial u_x}{\partial y},$$

$$e_{xx}=\frac{\partial u_x}{\partial x},e_{yy}=\frac{\partial u_y}{\partial y},e_{zz}=\frac{\partial u_z}{\partial z} \qquad (10)$$

components of the small deformation tensor [24, 25]. Taking into account (10), the components of the stress tensor can be written as follows:

$$\sigma_{xx}=\lambda\left[\frac{\partial}{\partial x}\left(\frac{\partial\varphi}{\partial x}+\frac{\partial\psi_z}{\partial y}-\frac{\partial\psi_y}{\partial z}\right)+\frac{\partial}{\partial y}\left(\frac{\partial\varphi}{\partial y}+\frac{\partial\psi_z}{\partial x}-\frac{\partial\psi_x}{\partial z}\right)\right]+$$

$$+\lambda\left[\frac{\partial}{\partial z}\left(\frac{\partial\varphi}{\partial z}+\frac{\partial\varphi_y}{\partial x}-\frac{\partial\psi_x}{\partial y}\right)\right]+2\mu\frac{\partial}{\partial x}\left(\frac{\partial\varphi}{\partial x}+\frac{\partial\psi_z}{\partial y}-\frac{\partial\psi_y}{\partial z}\right)=$$

$$=\lambda\left[\Delta\varphi+2\left(\frac{\partial^2\psi_z}{\partial x\partial y}-\frac{\partial^2\psi_x}{\partial y\partial z}\right)\right]+2\mu\left(\frac{\partial^2\varphi}{\partial x^2}+\frac{\partial^2\psi_z}{\partial x\partial y}-\frac{\partial^2\psi_y}{\partial x\partial z}\right),$$

$$\sigma_{yy}=\lambda\left[\frac{\partial^2\varphi}{\partial x^2}+\frac{\partial^2\psi_z}{\partial x\partial y}-\frac{\partial^2\psi_y}{\partial x\partial z}+\frac{\partial^2\varphi}{\partial y^2}+\frac{\partial^2\psi_z}{\partial y\partial x}-\frac{\partial^2\psi_x}{\partial y\partial z}\right]+$$

$$+\left[\frac{\partial^2\varphi}{\partial z^2}+\frac{\partial^2\psi_y}{\partial z\partial x}-\frac{\partial^2\psi_x}{\partial z\partial y}\right]+2\mu\frac{\partial}{\partial y}\left(\frac{\partial\varphi}{\partial y}+\frac{\partial\psi_z}{\partial x}-\frac{\partial\psi_x}{\partial z}\right)=$$

$$=\lambda\left[\Delta\varphi+2\left(\frac{\partial^2\psi_z}{\partial x\partial y}-\frac{\partial^2\psi_x}{\partial y\partial z}\right)\right]+2\mu\left(\frac{\partial^2\varphi}{\partial y^2}+\frac{\partial^2\psi_z}{\partial x\partial y}-\frac{\partial^2\psi_x}{\partial y\partial z}\right)=$$

$$=\lambda\Delta\varphi+2(\lambda+\mu)\left(\frac{\partial^2\psi_z}{\partial x\partial y}-\frac{\partial^2\psi_x}{\partial y\partial z}\right)+2\mu\frac{\partial^2\varphi}{\partial y^2},$$

$$\sigma_{zz}=\lambda\left[\Delta\varphi+2\left(\frac{\partial^2\psi_z}{\partial x\partial y}-\frac{\partial^2\psi_x}{\partial y\partial z}\right)\right]+2\mu\frac{\partial}{\partial z}\left(\frac{\partial\varphi}{\partial z}+\frac{\partial\psi_y}{\partial x}-\frac{\partial\psi_x}{\partial y}\right)=$$

$$=\lambda\left[\Delta\varphi+2\left(\frac{\partial^2\psi_z}{\partial x\partial y}-\frac{\partial^2\psi_x}{\partial y\partial z}\right)\right]+2\mu\left(\frac{\partial^2\varphi}{\partial z^2}+\frac{\partial^2\psi_y}{\partial x\partial z}-\frac{\partial^2\psi_x}{\partial z\partial y}\right)=$$

$$=\lambda\left[\Delta\varphi+2\frac{\partial^2\psi_z}{\partial x\partial y}\right]-2(\lambda+\mu)\frac{\partial^2\psi_x}{\partial y\partial z}+2\mu\left(\frac{\partial^2\varphi}{\partial z^2}+\frac{\partial^2\psi_y}{\partial x\partial z}\right),$$

$$\sigma_{yz}=\mu\left[\frac{\partial}{\partial y}\left(\frac{\partial\varphi}{\partial z}+\frac{\partial\psi_y}{\partial x}-\frac{\partial\psi_x}{\partial y}\right)+\frac{\partial}{\partial z}\left(\frac{\partial\varphi}{\partial y}+\frac{\partial\psi_z}{\partial x}-\frac{\partial\psi_x}{\partial z}\right)\right]=$$

$$=\mu\left[\frac{\partial^2\varphi}{\partial y\partial z}+\frac{\partial^2\psi_y}{\partial x\partial y}-\frac{\partial^2\psi_x}{\partial y^2}+\frac{\partial^2\varphi}{\partial z\partial y}+\frac{\partial^2\psi_z}{\partial z\partial x}-\frac{\partial^2\psi_x}{\partial z^2}\right]=$$

$$=\mu\left[2\frac{\partial^2\varphi}{\partial y\partial z}+\frac{\partial^2\psi_y}{\partial x\partial y}-\frac{\partial^2\psi_x}{\partial y^2}-\frac{\partial^2\psi_x}{\partial z^2}+2\frac{\partial^2\psi_z}{\partial z\partial x}\right],$$

$$\sigma_{xz}=\mu\left[\frac{\partial}{\partial x}\left(\frac{\partial\varphi}{\partial z}+\frac{\partial\psi_y}{\partial x}-\frac{\partial\psi_x}{\partial y}\right)+\frac{\partial}{\partial z}\left(\frac{\partial\varphi}{\partial x}+\frac{\partial\psi_z}{\partial y}-\frac{\partial\psi_y}{\partial z}\right)\right]=$$

$$=\mu\left[\frac{\partial^2\varphi}{\partial x\partial z}+\frac{\partial^2\psi_y}{\partial x^2}-\frac{\partial^2\psi_x}{\partial x\partial y}+\frac{\partial^2\varphi}{\partial z\partial x}+\frac{\partial^2\psi_z}{\partial z\partial y}-\frac{\partial^2\psi_y}{\partial z^2}\right]=$$

ISSN 1814-4225 (print)
ISSN 2663-2012 (online)

$$= \mu\left[2\frac{\partial^2\varphi}{\partial x\partial z} + \frac{\partial^2\psi_y}{\partial x^2} - \frac{\partial^2\psi_y}{\partial z^2} + \frac{\partial^2\psi_z}{\partial z\partial y} - \frac{\partial^2\psi_x}{\partial x\partial y}\right],$$

$$\sigma_{xy} = \mu\left[\frac{\partial}{\partial x}\left(\frac{\partial\varphi}{\partial y} + \frac{\partial\psi_z}{\partial x} - \frac{\partial\psi_x}{\partial z}\right) + \frac{\partial}{\partial y}\left(\frac{\partial\varphi}{\partial x} + \frac{\partial\psi_z}{\partial y} - \frac{\partial\psi_y}{\partial z}\right)\right] =$$

$$= \mu\left[\frac{\partial^2\varphi}{\partial x\partial y} + \frac{\partial\psi_z}{\partial x^2} - \frac{\partial^2\psi_x}{\partial x\partial z} + \frac{\partial^2\varphi}{\partial y\partial x} + \frac{\partial^2\psi_z}{\partial y^2} - \frac{\partial^2\psi_y}{\partial y\partial z}\right] =$$

$$= \mu\left[2\frac{\partial^2\varphi}{\partial x\partial y} + \frac{\partial^2\psi_z}{\partial x^2} - \frac{\partial^2\psi_x}{\partial x\partial z} + \frac{\partial^2\psi_z}{\partial y^2} - \frac{\partial^2\psi_y}{\partial y\partial z}\right]. \quad (11)$$

Now, using the representation of the stress tensor component, we formulate the boundary conditions.

4. Boundary conditions

1. The free boundary condition (Fig. 2) means zero stress. The condition applies to the blade ends:

– at the border $y = 0,\ y = R$:

$$\sigma_{yx} = 0,\ \sigma_{yy} = 0,\ \sigma_{yz} = 0, \quad (12)$$

– at the border $x = 0,\ x = c$:

$$\sigma_{xx} = 0,\ \sigma_{zx} = 0,\ \sigma_{yx} = 0. \quad (13)$$

2. On the surfaces of the blades $z = \pm h$:

$$\sigma_{zz} = -q(x,y),\ \sigma_{xz} = 0,\ \sigma_{yz} = 0,\ u_z = 0. \quad (14)$$

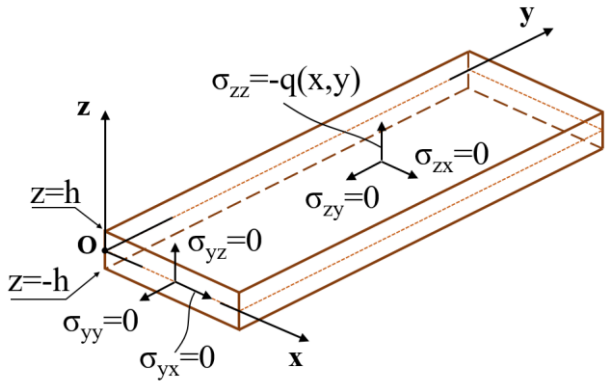

Fig. 2. Boundary conditions on the surface of the plate

5. General solution of equations (6)

Let us solve the equation for the potential using the method of separation of variables. According to the method of separation of variables, we represent the potential as a product of functions:

$$\varphi(x,y,z) = X(x)Y(y)Z(z). \quad (15)$$

Substituting (15) into the first equation (6), we obtain:

$$\frac{X''(x)}{X(x)} + \frac{Y''(y)}{Y(y)} + \frac{Z''(z)}{Z(z)} + k_1^2 = 0. \quad (16)$$

Since each of the terms, except for k_1^2 , are functions of different coordinates, and k_1^2 is a constant, then

$$\frac{X''(x)}{X(x)} = -\lambda_1^2, \frac{Y''(y)}{Y(y)} = -\lambda_2^2,$$

$$\frac{Z''(z)}{Z(z)} = -\left(k_1^2 - \left(\frac{\pi k}{c}\right)^2 - \left(\frac{\pi n}{R}\right)^2\right). \quad (17)$$

Next, let's solve the problem for eigenvalues by coordinates x, y , i.e. we assume that

$$\varphi(0,y,z) = \varphi(c,y,z) = \varphi(x,0,z) = \varphi(x,R,z) = 0. \quad (18)$$

We can make this assumption approximately because we are considering small displacements determined by sound potentials. And we neglect the sound field at the ends of the blade accordingly. The solution for the function $X(x)$ has the general form:

$$X(x) = A\cos\lambda_1 x + B\sin\lambda_1 x, \quad (19)$$
$$X(0) = 0: A\cdot 1 + B\cdot 0 = 0, \Rightarrow A = 0,$$
$$X(c) = 0: B\sin\lambda_1 c = 0, B \neq 0, \Rightarrow \sin\lambda_1 c = 0.$$

$\lambda_1 = \frac{\pi k}{c}$, $k \in 0,1,2,...$ – are the eigenvalues.

Then

$$X(x) = B\sin\frac{\pi k}{c}x. \quad (20)$$

Accordingly $y = 0; R: Y(0) = Y(R) = 0$.

$$Y(y) = C\cos\lambda_2 y + D\sin\lambda_2 y,$$

$$C = 0,\ \lambda_2 = \frac{\pi n}{R},\ n \in 0,1,2,...$$

And then

$$Y(y) = D\sin\frac{\pi n}{R}y. \quad (21)$$

Stresses different from zero are specified on the upper and lower surfaces of the blade. We can find the

solution $Z(z)$ as follows. For numbers $n,k=0$, we have $X(x)=Y(y)=0$. Therefore, we finally have:

$$\varphi(x,y,z)=X\cdot Y\cdot Z= \\ =\sum_{k=1}^{\infty}\sum_{n=1}^{\infty}B_k\sin\frac{\pi k}{c}x\cdot D_n\sin\frac{\pi n}{R}y\cdot Z(z). \quad (22)$$

Substituting the simplified expression $\varphi(x,y,z)$ into equation (6), we obtain:

$$Z''(z)+\left(k_1{}^2-\left(\frac{\pi k}{c}\right)^2-\left(\frac{\pi n}{R}\right)^2\right)Z(z)=0. \quad (23)$$

However, analysis of the sign of the expression $k_1{}^2-\left(\frac{\pi k}{c}\right)^2-\left(\frac{\pi n}{R}\right)^2$ indicates that $k_1{}^2$ is significantly less than $\left(\frac{\pi k}{c}\right)^2-\left(\frac{\pi n}{R}\right)^2$ for all non-zero values k,n. Therefore, the only standing wave that can exist corresponds to the values $k=n=0$. But according to (22), we only have zero. Therefore, the only possible solution is:

$$Z(z)=A_{nk}\,ch t_{nk}z+B_{nk}\,sh t_{nk}z, \quad (24)$$

Ultimately, the expression for potential will take the form:

$$\varphi(x,y,z)=\sum_{k=1}^{\infty}\sum_{n=1}^{\infty}(A_{nk}\,ch t_{nk}z+B_{nk}\,sh t_{nk}z)\cdot \\ \cdot\sin\frac{\pi k}{c}x\cdot\sin\frac{\pi n}{R}y. \quad (25)$$

As we can see, we have not yet determined the unknown constants A_{nk},B_{nk}. They will be determined later, together with the unknown constants for the vector potential $\bar{\psi}(x,y,z)$ when performing the boundary condition on the blade surfaces.

Since the second equation of the system of equations (6) for the vector potential $\bar{\psi}(x,y,z)$ has the same form with an accuracy of the square of the wave vector k_t^2, its general solution for the three components can be written as follows:

$$\psi_x(x,y,z)=\sum_{k=1}^{\infty}\sum_{n=1}^{\infty}(C_{nk}\,ch p_{nk}z+D_{nk}\,sh p_{nk}z)\cdot \\ \cdot\sin\frac{\pi k}{c}x\cdot\sin\frac{\pi n}{R}y,$$

$$\psi_y(x,y,z)=\sum_{k=1}^{\infty}\sum_{n=1}^{\infty}(F_{nk}\,ch p_{nk}z+E_{nk}\,sh p_{nk}z)\cdot \\ \cdot\sin\frac{\pi k}{c}x\cdot\sin\frac{\pi n}{R}y,$$

$$\psi_z(x,y,z)=\sum_{k=1}^{\infty}\sum_{n=1}^{\infty}(G_{nk}\,ch p_{nk}z+L_{nk}\,sh p_{nk}z)\cdot \\ \cdot\sin\frac{\pi k}{c}x\cdot\sin\frac{\pi n}{R}y, \quad (26)$$

where

$$p_{nk_{1,2}}=\sqrt{-k_t{}^2+\left(\frac{\pi k}{c}\right)^2+\left(\frac{\pi n}{R}\right)^2}.$$

Thus, we have a general solution for both scalar and vector potentials. It remains to find the unknown constants A_{nk},B_{nk}, C_{nk},D_{nk}, F_{nk},E_{nk}, G_{nk},L_{nk}. Note that we actually used boundary conditions (12)-(13) when finding eigenvalues for the scalar and vector potentials, equating them to zero. Since, according to (11), the components of the stress tensor are expressed in terms of potentials that are zero at the ends, the stresses are also zero. Only the normal stresses $\sigma_{zz}=-q(x,y)$ are non-zero.

Next, we will apply an unusual approach. Usually, the number of unknown constants must correspond to the number of boundary conditions. However, from the zero boundary conditions for $\sigma_{xz}=0,\sigma_{yz}=0,u_z=0$ we can find a linearly dependent or trivial, i.e. zero, solution, since we have a linear system of algebraic equations with a zero right-hand side:

$$\sigma_{zx|z=\pm h}=\mu\left[2\frac{\pi n}{c}t_{nk}\sum_{n=1}^{\infty}\sum_{k=1}^{\infty}Z_1(\pm h)\times\sin\frac{\pi n}{R}y\cos\frac{\pi k}{c}x\right]- \\ -\mu\left[\left(\frac{\pi k}{c}\right)^2\sum_{n=1}^{\infty}\sum_{k=1}^{\infty}Z_2(\pm h)\times\sin\frac{\pi n}{R}y\sin\frac{\pi k}{c}x\right]- \\ -\mu\left[p_{nk}{}^2\sum_{n=1}^{\infty}\sum_{k=1}^{\infty}Z_2(\pm h)\times\sin\frac{\pi n}{R}y\sin\frac{\pi k}{c}x\right]+ \\ +\mu\left[p_{nk}\frac{\pi n}{R}\sum_{n=1}^{\infty}\sum_{k=1}^{\infty}Z_3(\pm h)\times\cos\frac{\pi n}{R}y\sin\frac{\pi k}{c}x\right]- \\ -\mu\left[\frac{\pi n}{R}\frac{\pi k}{c}\sum_{n=1}^{\infty}\sum_{k=1}^{\infty}Z_4(\pm h)\times\cos\frac{\pi n}{R}y\cos\frac{\pi k}{c}x\right]=0, \quad (27)$$

$$\sigma_{zy|z=\pm h}=\mu\left[2\frac{\pi n}{R}t_{nk}\sum_{n=1}^{\infty}\sum_{k=1}^{\infty}Z_1(\pm h)\times\cos\frac{\pi n}{R}y\sin\frac{\pi k}{c}x\right]+$$

ISSN 1814-4225 (print)
ISSN 2663-2012 (online)

$$+\mu\left[\frac{\pi n}{R}\frac{\pi k}{c}\sum_{n=1}^{\infty}\sum_{k=1}^{\infty}Z_2(\pm h)\times\cos\frac{\pi n}{R}y\cos\frac{\pi k}{c}x\right]+$$
$$+\mu\left[\left(\frac{\pi n}{R}\right)^2\sum_{n=1}^{\infty}\sum_{k=1}^{\infty}Z_4(\pm h)\times\sin\frac{\pi n}{R}y\sin\frac{\pi k}{c}x\right]+$$
$$+\mu\left[p_{nk}{}^2\sum_{n=1}^{\infty}\sum_{k=1}^{\infty}Z_4(\pm h)\times\sin\frac{\pi n}{R}y\sin\frac{\pi k}{c}x\right]+$$
$$+\mu\left[p_{nk}\frac{\pi k}{c}\sum_{n=1}^{\infty}\sum_{k=1}^{\infty}Z_3(\pm h)\times\sin\frac{\pi n}{R}y\cos\frac{\pi k}{c}x\right]=0\ ,(28)$$

$$\sigma_{zz|z=\pm h}=\lambda\left[-k_1{}^2\sum_{k=1}^{\infty}\sum_{n=1}^{\infty}Z_5(\pm h)\sin\frac{\pi k}{c}x\cdot\sin\frac{\pi n}{R}y\right]+$$
$$+\lambda\left[2\frac{\pi n}{R}\frac{\pi k}{c}\sum_{n=1}^{\infty}\sum_{k=1}^{\infty}Z_6(\pm h)\times\cos\frac{\pi n}{R}y\cos\frac{\pi k}{c}x\right]+$$
$$-2(\lambda+\mu)\left[\sum_{n=1}^{\infty}\sum_{k=1}^{\infty}Z_7(\pm h)\times\cos\frac{\pi n}{R}y\sin\frac{\pi k}{c}x\right]+$$
$$+2\mu\left[-t_{nk}{}^2\sum_{k=1}^{\infty}\sum_{n=1}^{\infty}Z_5(\pm h)\sin\frac{\pi k}{c}x\cdot\sin\frac{\pi n}{R}y\right]+$$
$$+2\mu\left[p_{nk}\frac{\pi k}{c}\sum_{n=1}^{\infty}\sum_{k=1}^{\infty}Z_8(\pm h)\times\sin\frac{\pi n}{R}y\cos\frac{\pi k}{c}x\right]=0\ ,\quad(29)$$

$$u_{z|z=\pm h}=p_{nk}\sum_{n=1}^{\infty}\sum_{k=1}^{\infty}Z_1(\pm h)\times\sin\frac{\pi n}{R}y\sin\frac{\pi n}{c}x+$$
$$+\frac{\pi k}{c}\sum_{n=1}^{\infty}\sum_{k=1}^{\infty}Z_2(\pm h)\times\sin\frac{\pi n}{R}y\cos\frac{\pi k}{c}x-$$
$$-\frac{\pi n}{R}\sum_{n=1}^{\infty}\sum_{k=1}^{\infty}Z_4(\pm h)\times\cos\frac{\pi n}{R}y\sin\frac{\pi k}{c}x=0\ .\quad(30)$$

In expressions (27)-(30), the following are denoted:

$$Z_1(\pm h)=-A_{nk}\,sht_{nk}(\pm h)+B_{nk}\,cht_{nk}(\pm h),$$
$$Z_2(\pm h)=F_{nk}\,chp_{nk}(\pm h)+E_{nk}\,shp_{nk}(\pm h),$$
$$Z_3(\pm h)=-G_{nk}\,shp_{nk}(\pm h)+L_{nk}\,chp_{nk}(\pm h),$$
$$Z_4(\pm h)=C_{nk}\,chp_{nk}(\pm h)+D_{nk}\,shp_{nk}(\pm h),$$
$$Z_5(\pm h)=A_{nk}cht_{nk}(\pm h)+B_{nk}sht_{nk}(\pm h)$$
$$Z_6(\pm h)=G_{nk}chp_{nk}(\pm h)+L_{nk}shp_{nk}(\pm h),$$
$$Z_7(\pm h)=-C_{nk}shp_{nk}(\pm h)+D_{nk}chp_{nk}(\pm h),$$
$$Z_8(\pm h)=-F_{nk}shp_{nk}(\pm h)+E_{nk}chp_{nk}(\pm h).$$

What should we do in this situation? Let's use the orthogonality of the trigonometric function system. This property will allow us to use only the boundary condition $\sigma_{zz}=-q(x,y)$ to determine the unknown constants.

Indeed, equation (29) contains all eight unknown constants $A_{nk},B_{nk},C_{nk},D_{nk},F_{nk},E_{nk},G_{nk},L_{nk}$. The orthogonality property of the trigonometric function system will give us non-zero coefficients only for those basis functions that we multiply and integrate over $0\le x\le c, 0\le y\le R$. We will find the unknown coefficients step by step:

Step 1: multiply (29) by $\sin\frac{\pi n}{R}y\sin\frac{\pi k}{c}x$ and integrate over the intervals $0\le x\le c,\ 0\le y\le R$:

$$\left(-\lambda k_1{}^2-2\mu t_{nk}{}^2\right)Z_5(\pm h)\cdot\frac{R}{2}\cdot\frac{c}{2}=$$
$$=-\int_0^c\int_0^R\begin{Bmatrix}q_{up}(x,y)\\q_{low}(x,y)\end{Bmatrix}\sin\frac{\pi n}{R}y\sin\frac{\pi k}{c}x\,dxdy=\begin{Bmatrix}\omega_1\\\omega_2\end{Bmatrix},\quad(31)$$

$$A_{nk}\,cht_{nk}h+B_{nk}\,sht_{nk}h=\frac{4\omega_1}{Rc\left(\lambda k_1{}^2+2\mu t_{nk}{}^2\right)},\quad(32)$$

$$A_{nk}\,cht_{nk}h-B_{nk}\,sht_{nk}h=\frac{4\omega_2}{Rc\left(\lambda k_1{}^2+2\mu t_{nk}{}^2\right)}.\quad(33)$$

Adding and subtracting (32) and (33) will give us the following:

$$A_{nk}=\frac{4(\omega_1+\omega_2)}{R\cdot c\cdot cht_{nk}h\left(\lambda k_1{}^2+2\mu t_{nk}{}^2\right)},$$
$$B_{nk}=\frac{4(\omega_1-\omega_2)}{R\cdot c\cdot sht_{nk}h\left(\lambda k_1{}^2+2\mu t_{nk}{}^2\right)}.\quad(34)$$

Step 2: Multiply (29) by $\cos\frac{\pi n}{R}y\sin\frac{\pi k}{c}x$ and integrate over the intervals $0\le x\le c, 0\le y\le R$. As a result, we have:

$$-2(\lambda+\mu)p_{nk}\left(\frac{\pi n}{R}\right)\left(-C_{nk}\,shp_{nk}(\pm h)+D_{nk}\,chp_{nk}(\pm h)\right)=$$
$$-\int_0^c\int_0^R\cos\frac{\pi n}{R}y\sin\frac{\pi n}{c}x\begin{Bmatrix}q_{up}(x,y)\\q_{low}(x,y)\end{Bmatrix}dxdy=-\begin{Bmatrix}\omega_5\\\omega_6\end{Bmatrix}.\quad(35)$$

$$2(\lambda+\mu)p_{nk}\left(\frac{\pi n}{R}\right)\cdot$$
$$\cdot\left(-C_{nk}\,shp_{nk}h+D_{nk}\,chp_{nk}h\right)=\omega_5,\quad(36)$$

$$2(\lambda+\mu)p_{nk}\left(\frac{\pi n}{R}\right)\cdot$$
$$\cdot\left(C_{nk}\,sh p_{nk}h + D_{nk}\,ch p_{nk}h\right) = \omega_6, \qquad (37)$$

$$C_{nk} = \frac{\omega_6-\omega_5}{4(\lambda+\mu)p_{nk}\left(\frac{\pi n}{R}\right)sh p_{nk}h},$$
$$D_{nk} = \frac{\omega_5+\omega_6}{4(\lambda+\mu)p_{nk}\left(\frac{\pi n}{R}\right)ch p_{nk}h}. \qquad (38)$$

Step 3: Multiply (29) by $\cos\frac{\pi n}{R}y\cos\frac{\pi k}{c}x$ and integrate over the intervals $0\le x\le c, 0\le y\le R$. As a result, we have:

$$2\lambda\left(\frac{\pi n}{R}\right)\left(\frac{\pi k}{c}\right)\frac{R}{2}\cdot\frac{c}{2}\left(G_{nk}\,ch p_{nk}(\pm h)+L_{nk}\,sh p_{nk}(\pm h)\right)=$$
$$=-\int_0^c\int_0^R\begin{Bmatrix}q_{up}(x,y)\\ q_{low}(x,y)\end{Bmatrix}\cos\frac{\pi n}{R}y\cos\frac{\pi k}{c}x\,dxdy=\begin{Bmatrix}\omega_3\\ \omega_4\end{Bmatrix}, \qquad (39)$$

Or

$$\frac{\lambda\pi^2 nk}{2}\left(G_{nk}\,ch p_{nk}(\pm h)+L_{nk}\,sh p_{nk}(\pm h)\right)=\begin{Bmatrix}\omega_3\\ \omega_4\end{Bmatrix}, \qquad (40)$$

$$G_{nk}\,ch p_{nk}h + L_{nk}\,sh p_{nk}h = \frac{2\omega_3}{\lambda\pi^2 nk},$$
$$G_{nk}\,ch p_{nk}h - L_{nk}\,sh p_{nk}h = \frac{2\omega_4}{\lambda\pi^2 nk}, \qquad (41)$$

$$G_{nk} = \frac{\omega_3+\omega_4}{\lambda\pi^2 nk\,ch p_{nk}h},$$
$$L_{nk} = \frac{\omega_3-\omega_4}{\lambda\pi^2 nk\,sh p_{nk}h}. \qquad (42)$$

Step 4: Multiply (29) by $\sin\frac{\pi n}{R}y\cos\frac{\pi k}{c}x$ and integrate over the intervals $0\le x\le c, 0\le y\le R$. As a result, we have:

$$\left(\frac{\pi k}{c}\right)\left(-F_{nk}\,sh p_{nk}(\pm h)+E_{nk}\,ch p_{nk}(\pm h)\right)\times\frac{R}{2}\cdot\frac{c}{2}=$$
$$=-\int_0^c\int_0^R\sin\frac{\pi n}{R}y\sin\frac{\pi k}{c}\begin{Bmatrix}q_{up}(x,y)\\ q_{low}(x,y)\end{Bmatrix}dxdy=-\begin{Bmatrix}\omega_7\\ \omega_8\end{Bmatrix}, \qquad (43)$$

$$-F_{nk}\,sh p_{nk}h + E_{nk}\,ch p_{nk}h = \frac{2\omega_7}{\mu p_{nk}\pi kR}, \qquad (44)$$

$$F_{nk}\,sh p_{nk}h + E_{nk}\,ch p_{nk}h = \frac{2\omega_8}{\mu p_{nk}\pi kR}, \qquad (45)$$

$$E_{nk} = \frac{\omega_7+\omega_8}{\mu p_{nk}\pi kR\,ch p_{nk}h},$$
$$F_{nk} = \frac{\omega_8-\omega_7}{\mu p_{nk}\pi kR\,sh p_{nk}h}. \qquad (46)$$

Thus, all unknown coefficients in the expressions for scalar and vector potentials have been found. Let us write down the final expressions for the scalar potential φ and the components of the vector potential $\bar{\psi}$:

$$\varphi(x,y,z)=4\sum_{k=1}^{\infty}\sum_{n=1}^{\infty}\frac{(\omega_1+\omega_2)sh t_{nk}h\cdot ch t_{nk}z}{R\cdot c\cdot a_{nk}\cdot sh t_{nk}h\cdot ch t_{nk}h}\cdot$$
$$\cdot\sin\frac{\pi k}{c}x\cdot\sin\frac{\pi n}{R}y+$$
$$+4\sum_{k=1}^{\infty}\sum_{n=1}^{\infty}\frac{(\omega_1-\omega_2)ch t_{nk}h\cdot sh t_{nk}z}{R\cdot c\cdot a_{nk}\cdot sh t_{nk}h\cdot ch t_{nk}h}\cdot$$
$$\cdot\sin\frac{\pi k}{c}x\cdot\sin\frac{\pi n}{R}y, \qquad (47)$$

$$\psi_x(x,y,z)=\frac{1}{4}\sum_{k=1}^{\infty}\sum_{n=1}^{\infty}\frac{(\omega_6-\omega_5)chp_{nk}h\,ch p_{nk}z}{(\lambda+\mu)p_{nk}\left(\frac{\pi n}{R}\right)sh p_{nk}h\cdot chp_{nk}h}\cdot$$
$$\cdot\sin\frac{\pi k}{c}x\cdot\sin\frac{\pi n}{R}y+$$
$$+\frac{1}{4}\sum_{k=1}^{\infty}\sum_{n=1}^{\infty}\frac{(\omega_5+\omega_6)sh p_{nk}h\,sh p_{nk}z}{(\lambda+\mu)p_{nk}\left(\frac{\pi n}{R}\right)sh p_{nk}h\cdot chp_{nk}h}\cdot$$
$$\cdot\sin\frac{\pi k}{c}x\cdot\sin\frac{\pi n}{R}y. \qquad (48)$$

$$\psi_y(x,y,z)=\sum_{k=1}^{\infty}\sum_{n=1}^{\infty}\frac{(\omega_7+\omega_8)sh p_{nk}h\cdot ch p_{nk}z}{\mu p_{nk}\pi kR\,ch p_{nk}h\,sh p_{nk}h}\cdot$$
$$\cdot\sin\frac{\pi k}{c}x\cdot\sin\frac{\pi n}{R}y+$$
$$+\sum_{k=1}^{\infty}\sum_{n=1}^{\infty}\frac{(\omega_8-\omega_7)ch p_{nk}h\cdot sh p_{nk}z}{\mu p_{nk}\pi kR\,ch p_{nk}h\,sh p_{nk}h}\cdot$$
$$\cdot\sin\frac{\pi k}{c}x\cdot\sin\frac{\pi n}{R}y. \qquad (49)$$

ISSN 1814-4225 (print)
ISSN 2663-2012 (online)

$$\psi_z(x,y,z)=\sum_{k=1}^{\infty}\sum_{n=1}^{\infty}\frac{(\omega_3+\omega_4)\,sh p_{nk}h\cdot ch p_{nk}z}{\lambda\pi^2 nk\,ch p_{nk}h\,sh p_{nk}h}\cdot$$
$$\cdot\sin\frac{\pi k}{c}x\cdot\sin\frac{\pi n}{R}y+$$
$$+\sum_{k=1}^{\infty}\sum_{n=1}^{\infty}\frac{(\omega_3-\omega_4)\,ch p_{nk}h\cdot sh p_{nk}z}{\lambda\pi^2 nk\,ch p_{nk}h\,sh p_{nk}h}\cdot \qquad (50)$$
$$\cdot\sin\frac{\pi k}{c}x\cdot\sin\frac{\pi n}{R}y.$$

Expressions (47)-(50) are the solution to Navier-Cauchy equations (6) in the form of potentials describing standing waves along two coordinates x,y in a thin plate. With the coordinate z, as shown above, the roots t_{nk},p_{nk} of the corresponding characteristic equations gave us the dependence of potentials in the form of hyperbolic functions. But we are interested in the potential $\varphi(x,y,z)$ at the boundaries $z=\pm h$:

$$\varphi(x,y,h)=4\sum_{k=1}^{\infty}\sum_{n=1}^{\infty}\frac{2\omega_1}{R\cdot c\cdot\left(\lambda k_l{}^2+2\mu t_{nk}{}^2\right)}\cdot$$
$$\cdot\sin\frac{\pi k}{c}x\cdot\sin\frac{\pi n}{R}y,$$
$$\varphi(x,y,-h)=4\sum_{k=1}^{\infty}\sum_{n=1}^{\infty}\frac{2\omega_2}{R\cdot c\cdot\left(\lambda k_l{}^2+2\mu t_{nk}{}^2\right)}\cdot \qquad (51)$$
$$\cdot\sin\frac{\pi k}{c}x\cdot\sin\frac{\pi n}{R}y.$$

Expressions (51) are the amplitude distribution of longitudinal waves on the surfaces of the rotor blade. These waves are the source of vibration-induced sound, and the helicopter rotor blade, which we approximate with a thin rectangular plate, acts as a longitudinal wave emitter. The issue of reflection and scattering of part of the energy of sound waves at the boundary between two media, 'elastic plate - air,' is not studied in this work. Let us give a numerical calculation of the potential φ according to (51).

6. Numerical calculation of vibration noise

Expression (51) does not directly take into account the distribution of the sound wave amplitude over time, but only expressions $k_l{}^2, t_{nk}{}^2$ depend on frequency ω, since our process is harmonic over time. It is known that standing waves can form when the linear dimension of the object where the waves propagate is a multiple of the integer wavelength. Therefore, to determine how many terms of series (51) for each of the coordinates x,y to leave for numerical calculation, we will apply the known relationship between the linear dimension l, wavelength λ, and speed of sound c_{sd}: $l=n\cdot\lambda$, where $\lambda=c_{sd}/f$, or $n=l\cdot f/c_{sd}$. Let us take a simplified distribution of the load on the blade, which depends only on the coordinate y (Fig. 3). Using this relationship, and taking into account the frequency range of sound waves, we can approximately determine the number of standing waves along each of the coordinates x,y.

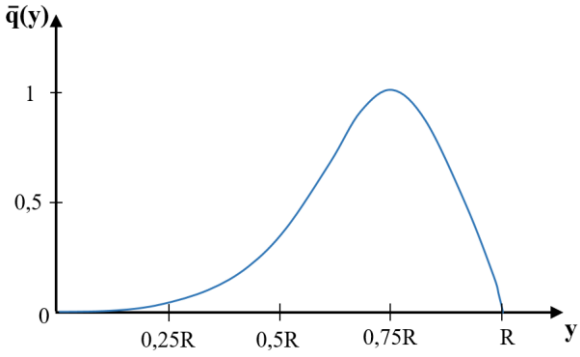

Fig. 3 Model distribution of aerodynamic load

Figs. 4, 5 shows the potential $\varphi(x,y)$ distribution data on the surface of an aluminium blade. Taking into account the physical parameters of aluminium, the following number of series members (51) was taken for the blade $R=4m,5m$, $c=0.4m,0.5m$: $k=3,n=10$. The numerical calculation data (Figs. 4, 5) indicate that the maximum in the longitudinal sound wave on the blade surface is formed closer to the end of the blade, at a distance of approximately $0.8R$, and to the front edge of the blade. This result is consistent with the well-known Gutain theory [1] of rotation noise.

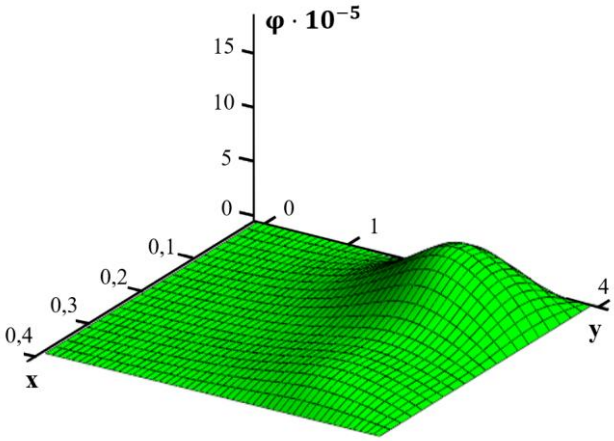

Fig. 4. Distribution of sound potential across the blade surface, m^2: $R=4m, c=0.4m$

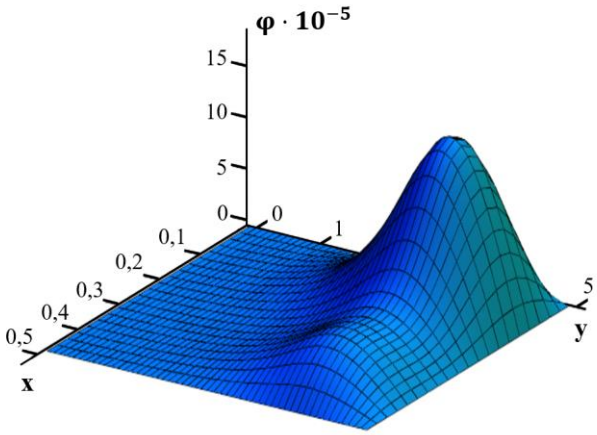

Fig. 5. Distribution of sound potential across the blade surface, m^2: $R = 5m, c = 0.5m$

Discussion

The analytical solution of the Navier-Cauchy equation for scalar and vector potentials allows us to investigate elastic standing waves formed in a thin rectangular plate. These waves emerge through the upper and lower parts of the blade in the form of sound vibrations. It should be noted that under the conditions of aerodynamic loading of the blade, we obtained the maximum values of the sound potential φ amplitude describing longitudinal waves at a distance of $0.8R$ from the outer end of the blade. This, firstly, corresponds to the known results according to Gutin's theory [1], and secondly, indicates that in the region of maximum aerodynamic loads on the blade, we have maximum generation of blade vibrations. The analytical expression of the longitudinal wave potential will be used in the future to calculate the far-field sound field of blade vibration noise.

Conclusions

This paper presents a new model for generating vibration-induced noise from helicopter blades. The blade is modelled as a thin, elastic, rectangular plate. It is assumed that under the action of aerodynamic load on the blade, the plate undergoes thickness deformation, which leads to the emergence of longitudinal and transverse sound waves in the middle of the blade. It is known that transverse waves do not propagate in liquid and gaseous media.

However, in an elastic body, longitudinal and shear waves are interconnected: the stresses that arise in the plate are functions of both scalar potential (longitudinal waves) and vector potential (shear waves). Therefore, on the blade surface, the distribution of normal stresses depends on the formation of longitudinal and shear waves.

Numerical calculations performed using the analytical solution obtained showed the physical proximity of the proposed model to the well-known Gutin rotation noise model. The analytical solution will be used in the future to calculate the far-field sound field of blade vibration noise.

Further research will focus on calculating the far sound field of a helicopter rotor using the theory proposed in this paper.

Contributions of authors: Problem formulation, physical model formulation, analytical solution of the problem, physical analysis of numerical calculations – **Petro Lukianov**; review of primary sources, numerical calculation of the problem, discussion of the physical model and results of numerical calculations, participation in writing the text of the article – **Sergii Karmazin**.

Conflict of Interest

The author declare that they have no conflict of interest in relation to this research, whether financial, personal, authorship or otherwise, that could affect the research and its results presented in this paper.

Financing

The research was conducted without financial support.

Data availability

The work has no associated data.

Use of Artificial Intelligence

The author confirms that he did not use artificial intelligence methods while creating the presented work

All authors have read and agreed to the publication of this version of the manuscript.

References

1. Gutin, L. *On the Sound Field of a Rotating Propeller*. NACA Technical Memorandum No.№1195, Washigton, 1948. 22 p. Available at: https://ntrs.nasa.gov/api/citations/20030068996/downloads/20030068996.pdf. (accessed 12.02.2025).

2. Lukianov, P. V. Ob odnoj modeli aeroakustiki vyazkogo szhimaemogo gaza. Chast I. Analiz sushestvuyushih modelej, vyvod sistemy reshaemyh uravnenij [On one model for aeroacousics of viscous compressible gas. Part I Analysis of existing models,dedusing of resolving system of equations]. *Akustychnyj visnyk - Acoustic bulletin*, 2013-2014, vol. 16, iss. 2, pp. 18-30. Available at: https://hydromech.org.ua/

ISSN 1814-4225 (print)
ISSN 2663-2012 (online)

content/pdf/av/av-16-2(18-30).pdf (accessed 12.02.2025). (In Russian).

3. Pulok, M. K. H., & Chakravarty, U. K. Aerodynamic and Vibration Analysis of a helicopter rotor blade. *Acta Mechanica*, 2024, vol. 235, pp. 3033-3037. DOI: 10.1007/s00707-024-03871-9.

4. Park, J. S. Simulteneous Vibration Reduction and Performance Improvement of Helicopter Rotor Using Individual Blade Pitch Control with Multiple Harmonic Inputs. *International Journal of Aeronautical and Space Sciences*, 2024, vol. 25, pp. 1330-1342. DOI: 10.1007/s42405-024-00744-2.

5. Oliveira, A. G., Silva, A. A., & et al. Helicopter vibration control employing superelastic pitch link with shape memory alloy. *Journal of Vibration and Control*, vol. 31, iss. 13-14, pp. 2676-2688. DOI: 10.1177/10775463241259568.

6. Li, S. K., & Lee, S. Analytic Prediction of Rotor Broadband Noise with Serrated Trailing Edges with Applications to Urban Air Mobility Aircraft. *Journal of American Helicopter Society*, 2024, vol. 69, iss. 3, pp. 1-14. DOI: 10.4050/JAHS.69.032005.

7. Singh, S. K., Shankar, G., Narayanmurthy, A., Baskaran, K., & Narayanan, S. Effect of sawtooth trailing edge serrations on the reductions of airfoil broadband noise. *International Journal of Aeroacoustics*, 2024, vol. 23, iss. 1-2, pp. 84–98. DOI: 10.1177/1475472X241226931.

8. Turhan, B., Jawahar, H. K., & et al. Acoustic characteristics of phase-synchronized adjacent propellers. *J. Acoust. Soc. Am.*, 2024, vol. 155, iss. 5, pp. 3242-3253. DOI: 10.1121/10.0025990.

9. Turhan, B., Jawahar, H. K., & et al. Characterizing the noise patterns of overlapping propellers in forward flight. *J. Acoust. Soc. Am*., 2025, vol. 157, iss. 4, pp. 2790-2801. DOI: 10.1121/10.0036453.

10. Akiwate, D. C., Joseph, P., & et al. On the balance between the tonal and broadband noise of isolated propellers. *International Journal of Aeroacoustics*, 2024, vol. 23, iss. 1-2, pp. 122–153. DOI: 10.1177/1475472X231225631.

11. Ulbricht, N., Boldini, A., Zhang, P., & Porfiri, M. Three-dimensional analytical solution of free vibrations of a simplt supported composite plate in contact with a fluid. *Journal of Sound and Vibration*, 2024, vol. 572, article no. 118139. DOI: 10.1016/j.jsv.2023.118139.

12. Aua, F. T. K., & Wang, M. F. Sound radiation from forced vibration of rectangular orthotropic plates under moving loads. *Journal of Sound And Vibration*, 2005, vol. 281, iss. 3-5, pp. 1057-1075, DOI: 10.1016%2Fj.jsv.2004.02.005.

13. Zhang, S., & Sheng, X. Analysis of sound transmission loss of a rectangular plate with acoustic treatments. *International conference on Noise and Vibration Engineering*, 2018, pp. 2275-2290. Available at: https://past.isma-isaac.be/downloads/isma2018/proceedings/Contribution_462_proceeding_3.pdf (accessed 12.02.2025).

14. Jorge, P. Arenas, Malcolm J. Crocker. Sound Radiation Efficiency of a Baffled Rectangular Plate Excited by Harmonic Point Forces Using its Surface Resistance Matrix. *International Jouranal of Acoustics amd Vibrations*, 2002, vol. 7, iss. 4, pp. 219-229. Available at: https://scispace.com/pdf/sound-radiation-efficiency-of-a-baffled-rectangular-plate-4zw2yxh3gc.pdf (accessed 12.02.2025).

15. Mattei, P.-O. Sound radiation by baffled and constrained plates. *Journal of Sound and Vibration*, 1995, vol. 179, iss. 7, pp. 63-77. DOI: 10.1006/jsvi.1995.0004.

16. Efimcev, B. M., & Zverev, A. Ya. Izluchenie zvuka plastinoj, svyazannoe s ee inercionnym povedeniem v neodnorodnov pole pulsacij davlenia [Sound radiation by a plate caused by its inertial behavior in a non-uniform pressure pulsation field]. *Uchyonye zapiski CAGI*, 2009, vol. 40, iss. 1, pp. 60-71. Available at: https://www.noisetp.com/media/filer_public/c9/21/c921d58d-de0d-4cc0-91f1-b307ba2592ec/noisetp2023issue2_9p19-28.pdf (accessed 12.02.2025). (In Russian).

17. Svetlov, V. V. Noise generation of the plate in the field of turbulent pressure pulsations. *NOISE Theory and Practice*, pp. 19-28. Available at: https://www.noisetp.com/media/filer_public/c9/21/c921d58d-de0d-4cc0-91f1-b307ba2592ec/noisetp2023issue2_9p19-28.pdf (accessed 12.02.2025). (In Russian).

18. Lamb, H. On waves on Elastic Plate. *Proceedings of the Royal Society of London*, Series A, 1917, vol. 93, iss. 648, pp. 114-128. DOI: 10.1098/rspa.1917.0008.

19. Viktorov, I. A. *Fizicheskie osnovy primeneniya ultazvukovyh voln Releya i Lemba v tehnike* [*Physical principles of the application of Rayleigh and Lamb ultrasonic waves in technology*]. Moscow, Publ. Nauka, 1968. 168 p. Available at: https://libarch.nmu.org.ua/handle/GenofondUA/67996 (accessed 12.02.2025). (In Russian).

20. Viktorov, I. V. *Zvukovye poverhnostnye volny v tverdyh telah* [Sound surface waves in solids]. Moscow, Publ. "Nauka". 1981. 287 p. DOI: 10.4050/JAHS.69.032005enofondUA/57041. (In Russian).

21. Grinchenko, V. T., & Meleshko, V. V. *Garmonicheskie kolebaniya i volny v uprugih telah* [Harmonic oscillations and waves in elastic bodies]. Kiev. Publ. "Naukova dumka". 1981. 284 p. Available at: https://libarch.nmu.org.ua/handle/GenofondUA/60725?locale-attribute=ru (accessed 12.02.2025). (In Russian).

22. Timoshenko, S. Woinowsky-Krieger. *Theory of Plates and Shells*. "MCGRAW-HILL BOOK COMPANY".1959. 594 p.

23. Isakovich**,** M. A. Obshaya akustika [*General Acoustics*]. Moscow, Publ.*"Science*", 1973.495 p. (In Russian).

24. Lependin, L. F. *Akustika* [*Acoustics*]. Moscow, Publ. "Vysshaya shkola", 1978. 448 p. (In Russian).

25. Lejbenzon, L. S. *Kurs teorii uprugosti* [*Course on elasticity theory*]. "OGIZ". 1947. 465 p. (In Russian).

Received 11.08.2025, Received in revised form 02.11.2025
Accepted date 17.11.2025, Published date 08.12.2025

ШУМ ПРУЖНИХ ТОВЩИННИХ КОЛИВАНЬ ЛОПАТІ ВЕРТОЛЬОТА, СПРИЧИНЕНИХ ДІЄЮ АЕРОДИНАМІЧНОГО НАВАНТАЖЕННЯ

П. В. Лук'янов, С. В. Кармазін

Предметом даної роботи є розробка теоретичної моделі генерації шуму пружних товщинних коливань лопатей вертольота, яка знаходиться під дією аеродинамічного навантаження. Цей шум разом із шумом аеродинамічного походження генерується під час обертання ротора вертольота. Шуму аеродинамічного походження присвячено чимало досліджень, запропоновано низку теорій. Однак, шум вібраційної природи досліджений в основному експериментально, або ж моделюється лише звичайними механічними коливанням лопаті як єдиного тіла - балки або пластини. При цьому не враховуються пружні деформації лопаті, які генерують пружні звукові хвилі усередині тіла. До сих пір не існувало моделі, яка здатна математично описати процес трансформації пружних поздовжніх та поперечних хвиль, що виникають всередині пружної лопаті, у звукові хвилі. Ці хвилі виходять з лопасті і поширюються у повітря під час пружних товщинних коливань, які утворюються змінними деформаціями лопаті під дією змінних навантажень на лопать. **Методи дослідження засновані на** на аналітичному розв'язку граничної задачі для рівняння Нав'є-Коші, яке розділяється на чотири рівняння Гельмгольца: одне рівняння для скалярного потенціалу та три рівняння для векторного потенціалу. Досліджуються пружні хвилі типу хвиль Лява, але для тонкої пружної пластини скінчених розмірів. Для лопаті ротора вертольота скінчених розмірів обмежитись стоячими хвилями лише в одному напрямку не можна, оскільки лопать має скінчені розміри. Тому, було запропоновано наступну модель виникнення вібраційного шуму. Лопать наближено замінено на тонку пружну пластину, усередені якої виникають пружні повздовжні та поперечні хвилі, які описуються рівняннями Гельмгольца. Загальний розв'язок даних рівнянь знайдено за допомогою методу розділення змінних (Фур'є). Питання відбиття та розсіювання звукових хвиль від поверхні розділу «пружне тіло – повітря» в роботі не розглядається. **Результати та висновки**. В роботі запропнованонову нову фізичну модель звуку вібраційного походження: звук вібраційного походження генерується як результат випромінювання пружних продольних хвиль, які випромінюються зсередини пружної лопаті назовні у повітря. Для граничної задачі з відомим розподілом аеродинамічного, гармонічного у часі, навантаження на поверхнях лопаті отримано аналітичний розв'язок скалярного та векторного потенціалів у вигляді стоячих звукових хвиль. Цей розв'язок дозволив записати вирази для нормальних напружень на поверхні лопаті. Змінні у часі напруження передають енергію повздовжніх стоячих звукових хвиль, які виходить з середини лопаті назовні у повітря. Вони і є джерелом шуму вібраційного походження. Вираз для нормальних напружень на поверхні лопаті містить у собі похідні як скалярного так і векторного потенціалу, тобто у ньому враховується вплив і повздовжніх і поперечних хвиль. Отже, обидва типи хвиль беруть участь у формуванні нормальних напружень на поверхні лопаті. Періодична зміна у часі цих напружень викликає періодичну товщинну деформацію лопаті, яка є джерелом акустичних коливань у повітрі. Дані розрахунку потенціалу повздовжньої хвилі на поверхні лопаті збігаються з теорією звуку обертання Гутіна: максимум у звуковій хвилі, що генерується, знаходиться поблизу зовнішнього кінця лопаті. А це свідчить про те, що отриманий розв'язок у даній роботі аналітичний розв'язок фізично описує процес генерації шуму вібраційного походження.

Ключові слова: модель шуму вібраційного походження; аеродинамічне наватаження на лопать вертольота; генерація пружних звукових хвиль на поверхні лопаті вертольота.

Лук'янов Петро Володимирович – канд. фіз.-мат. наук, старш. наук. співроб., зав. каф. авіа- та ракетобудування, Національний технічний університет України «КПІ ім.Ігоря Сікорського», Київ, Україна.

Сергій Кармазін – магістр, асп. каф. авіа- та ракетобудування, Національний технічний університет України "КПІ ім.Ігоря Сікорського", Київ, Україна.

Petro Lukianov – Candidate of Physics and Mathematics Sciences, Senior Researcher, Head of the Department of Avia- and Rocket Constructions, National Technical University of Ukraine "Igor Sikorsky Kyiv Polytechnic Institute", Kyiv, Ukraine, e-mail: p.lukianov@kpi.ua, ORCID: 0000-0002-7584-1491.

Sergii Karmazin – Master of Technical Sciences, PhD student of the Department of Avia- and Rocket Constructions, National Technical University of Ukraine "Igor Sikorsky Kyiv Polytechnic Institute", Kyiv, Ukraine, e-mail: idgbug@gmail.com, ORCID: 0000-0002-0033-2414.